Hyperfine Interactions 44 (1988) 125–138

PRODUCTION AND APPLICATIONS OF MONOENERGETIC POLARIZED POSITRON BEAMS

A. RICH, R.S. CONTI, D.W. GIDLEY, M. SKALSEY, J. VAN HOUSE and P.W. ZITZEWITZ *

Department of Physics, The University of Michigan, Ann Arbor, MI 48109, U.S.A.
** Department of Natural Sciences, The University of Michigan-Dearborn, Dearborn, MI 48128, U.S.A.*

The generation and applications of monoenergetic, high intensity, spin-polarized positron (e^+) beams are reviewed. Techniques for obtaining highly polarized beams are discussed. Applications include studies of surface and bulk magnetism, studies of optically active molecules, tests of discrete symmetries, and polarized antiproton production.

1. Introduction

Positrons (e^+) are emitted in the decay of a radioactive nucleus with net helicity as a result of parity non-conservation in the weak interaction. Moderation of these e^+ permits the production of spin-polarized low-energy (slow) e^+ beams [1,2].

With the exception of electron capture to form Ps (primarily a low incident energy phenomena), the positron interactions with a solid are relatively insensitive to e^+ spin.

This is because the repulsion of the e^+ from the atomic core reduces spin-orbit effects. In addition, the lack of identity with electrons eliminates the Pauli exclusion principle that causes large spin-dependent effects in electron scattering. As a result, the e^+ spin direction is largely preserved when the e^+ lose energy in non-magnetic moderators. [3]. This fact permits the easy production of polarized low-energy e^+ beams. Although the efficiency of existing moderators limits the beam intensities to a small fraction of the intensity of typical polarized electron beams, the efficiency of positron polarimeters [4] is of order 100 times larger than that of the standard electron polarimeter with similar or larger asymmetries possible (up to 26%). Thus precise measurements of e^+ polarization can be rapidly made. Spin-polarized slow e^+ beams have found a variety of applications in recent years. These include: studies of surface [5,6] and bulk [7] magnetism, studies of electron helicity density in optically active molecules [8], studies of slow e^+ emission from insulators [7], and tests of discrete symmetries using polarized Ps [9]. In the future we expect that the development of very intense polarized beams may allow the production of useful numbers of spin-polarized antiprotons.

2. Measuring positron polarization

The measurement of e^+ polarization [7] is based on the mixing of the singlet and the $m = 0$ triplet substates to form two field-perturbed states when Ps is produced in a magnetic field. The magnetic mixing not only increases the decay rate, λ', of the perturbed triplet state, but it also makes the fraction of Ps formed in this state dependent on the quantity $\boldsymbol{P} \cdot \hat{\boldsymbol{B}}$, where $\boldsymbol{P}$ is the positron polarization and $\hat{\boldsymbol{B}}$ is a unit vector in the direction of the magnetic field. The decay spectrum of oPs is given by

$$\frac{dN(t)}{dt} = \frac{N}{4}\left[2\lambda\, e^{-\lambda t} + (1 - \eta \boldsymbol{P} \cdot \hat{\boldsymbol{B}})\lambda' e^{-\lambda' t}\right].$$

Here N is the total number of Ps atoms formed and λ is the magnetically unperturbed ($m = \pm 1$) decay rate including all quenching mechanisms ($\lambda^{-1} \leqslant 142$ ns). The parameter η is given by $\eta = \chi/(1 + \chi^2)^{1/2}$, where $\chi = 0.276B$ for B in tesla. The perturbed decay rate is $\lambda' = (\lambda + y^2\lambda_s)/(1 + y^2)$, where $\lambda_s^{-1} = 0.125$ ns and $y = \chi/[1 + (1 + \chi^2)^{1/2}]$. For example at $B = 0.65$ T, one obtains $\eta = 0.176$ and $(\lambda')^{-1} = 15$ ns. Thus decays from the perturbed triplet state can be distinguished from decays from the unperturbed state by their much higher decay rate.

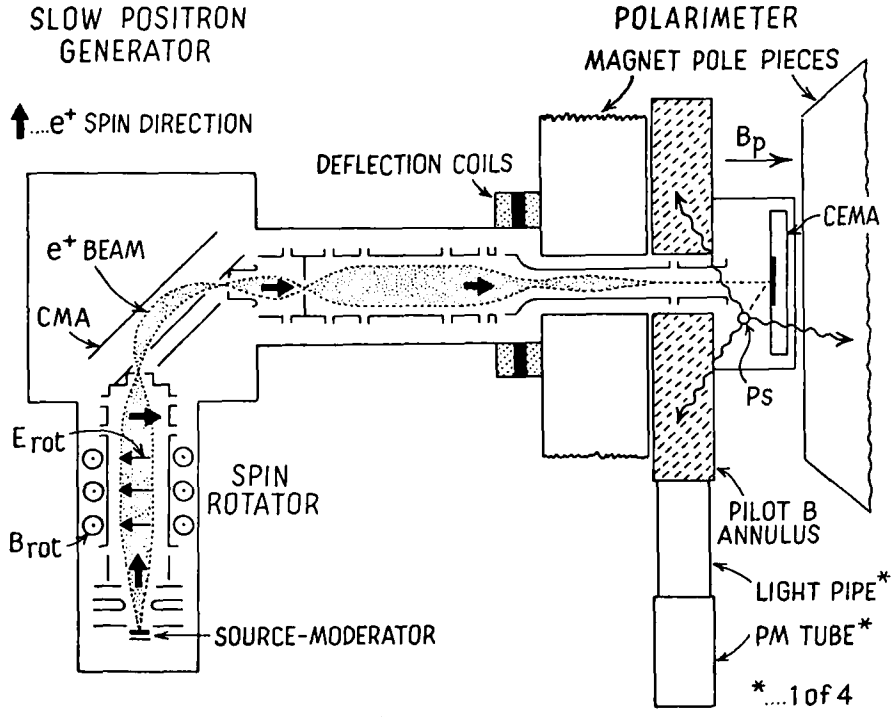

Fig. 1. Low-energy e^+ beam generator and polarimeter.

The quantity ηP can be determined by measuring changes in the intensity of the perturbed triplet component relative to the intensity of the unperturbed triplet component when the e^+ spin direction or the applied magnetic field direction is varied. The relative intensity is measured by recording annihilation events in the background-corrected decay spectrum in two separate time windows, the perturbed window W_1 (of which a fraction f are composed of decays from the perturbed triplet state), and the normalization window W_2 (composed 99% of unperturbed decays.) The ratio (R) of the number of counts in W_1 to W_2 is proportional to the perturbed triplet intensity. This ratio is formed first for $\boldsymbol{P}\cdot\hat{\boldsymbol{B}} > 0$ (R_+) and then, upon reversal of the direction of either $\boldsymbol{P}$ or $\hat{\boldsymbol{B}}$, for $\boldsymbol{P}\cdot\hat{\boldsymbol{B}} < 0$ (R_-). The e^+ polarization is then given by

$$P = \frac{1(R_- - R_+)}{\eta f(R_- + R_+)}.$$

In the Michigan polarized beam, an electrostatic system (fig. 1) accelerates, focuses, and transports the beam to a polarimeter. A Wien filter (crossed electric and magnetic fields) is used to rotate the e^+ spin directions without disturbing the particle motion. The e^+ beam is projected into the polarimeter and subsequently strikes a CEMA (chevron electron multiplier array) where the secondary electrons, generated by the impact of the 500 eV e^+, are collected to form a pulse that indicates the time of e^+ arrival and location of Ps formation. The annihilation γ-rays are detected in plastic scintillators coupled to four photomultipliers. The time between oPs formation and annihilation can be recorded with a conventional time-to-amplitude converter/multi-channel analyzer system. The lifetime of each oPs event is thus directly measured and recorded. Operation of the polarimeter is demonstrated by the spin-rotation curves shown in fig. 2.

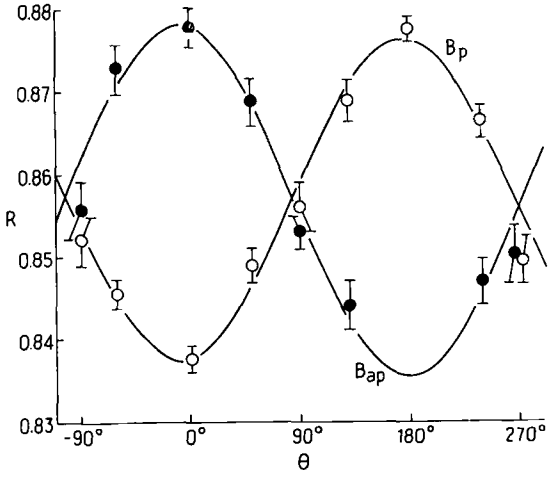

Fig. 2. Normalized perturbed oPs rate versus spin rotation angle. Curves are shown for $\boldsymbol{B}$ parallel and anti-parallel to beam velocity.

3. Producing a highly polarized beam

The polarization of the beam depends on the β^+ ensemble selected by the source and moderator, and on changes in the directions of β^+ spins caused by the passage of the particles through materials (including the moderator) or by stray magnetic fields. The ensemble selection includes both the angular spin distribution, determined by the angle between the emitted source β^+ and the beam axis, and the energy distribution. Polarization is reduced by introducing into the distribution β^+ backscattered from the source with reversed spin directions. Backscattering can be reduced by depositing the ^{22}Na on a low-Z material (e.g., Be). Beam polarization is increased when the low-energy, low-helicity β^+ from the source spectrum are absorbed in the source material, Ti source holder window, and any additional absorbers located between source and moderator. Absorbers also increase beam polarization by preferentially absorbing those source β^+ that are emitted at large angles relative to the axis, and thus have low polarization.

Depolarization can result from spin-orbit interactions that occur during the various scattering processes in the absorbers and moderator. The magnitude of the depolarization depends on the initial energy of the incident β^+ as well as the atomic number (Z) of the medium [7]. Depolarization is minimized by using low energy β^+ and low-Z materials.

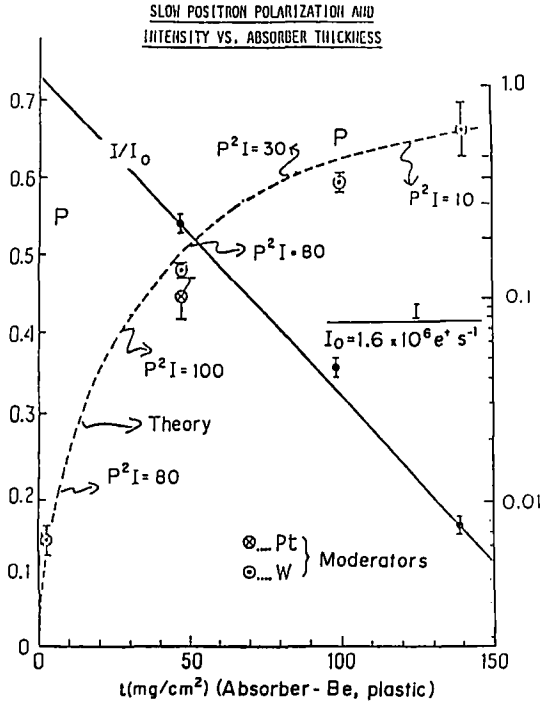

Fig. 3. Beam polarization and intensity versus absorber thickness. Dotted line shows theory [7]. Relative values of P^2I are shown at selected values of thickness.

The effect of low-Z (Be or plastic) absorbers on beam polarization is shown in fig. 3. While absorbers increase polarization for the reasons discussed above, they also reduce the intensity of the e^+ beam. The exponential attenuation length is (26.2 ± 0.4) mg/cm^2 for Be absorbers and a ^{22}Na source. Although beams with polarization as high as $P = 0.66 \pm 0.03$ have been produced, a beam that optimizes P^2I (where I is the beam intensity) has a polarization of about 0.45 and an net efficiency (slow e^+ in beam per source disintegration) of 3×10^{-4}. Thus, using a 47 mCi (1.7 GBq) ^{22}Na source, we obtain 5×10^5 e^+/s.

4. Applications of polarized low-energy positron beams

4.1. STUDIES OF THE POSITRON MODERATION PROCESS

As discussed above, high-energy β^+ are depolarized more by high-Z (Pt or W) moderators than by low-Z (MgO or Mo) moderators, while low-energy β^+ suffer no depolarization in any non-ferromagnetic material. Measurements of the polarization of a beam produced by moderators of different materials under otherwise identical conditions show that the beam polarization is independent of the moderator Z (fig. 4). Thus, we conclude that only β^+ incident on the moderator with very low energies are efficiently moderated. The uncertainty in the fitted slope of fig. 4 sets an energy upper limit for significant contribution to the beam of approximately 17 keV. The role of the low-Z absorbers in increasing

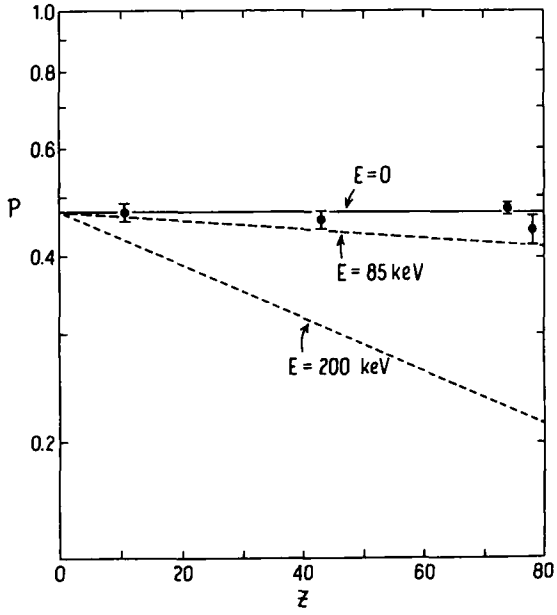

Fig. 4. Beam polarization versus moderator-Z. Dotted lines show theory [7] for two energies of incident e^+. Best fit is $E = (0 \pm 17)$ keV.

beam polarization is thus seen to be to reduce the energy of those β^+ emitted with high polarization to energies where they can be moderated efficiently without significant depolarization [7].

Polarization measurements can also be used to study the emission process of e^+ from insulating moderators such as MgO. Some models postulate the formation of Ps within the insulator, its escape, and subsequent ionization and release of the e^+. Depending on the lifetime of the postulated Ps, the e^+ polarization would be reduced to between 67% and 50% of its initial value by the spin randomization in the $m = 0$ state. The polarization of e^+ emitted from an MgO moderator is (within experimental error), however, the same as that of e^+ emitted from metallic moderators, indicating that the formation of Ps does not play a significant role in the emission of e^+ from MgO. Thus, theories of e^+ emission that involve an intermediate Ps state must account for this lack of depolarization.

4.2. STUDIES OF SURFACE MAGNETISM

Atoms at the surface or in a thin film of a metal have fewer neighbors than atoms in the bulk. As a result, their ferromagnetic behavior, a collective phenomenon, differs from that of atoms in the bulk. The investigation of surface and thin film magnetism tests our fundamental understanding of ferromagnetism and thus is a topic of active theoretical and experimental interest. The fact that Ps formation can occur only in the low-density tail of the electron distribution at the surface of a metal has been exploited by the Michigan-General Motors Research Laboratory group to study surface magnetism with polarized low-energy positrons [5,6].

The apparatus used to investigate surface magnetism is shown in fig. 5. The spin-polarized e^+ beam is similar to the ones discussed above except that is transversely polarized. The spin of the e^+ is rotated by $+90°$ (up) or $-90°$ (down) by an axial magnetic field before it enters the ultra high vacuum target chamber. The e^+ beam, at a selected energy between 300 and 1500 eV, is focused onto the surface of a Ni(110) single crystal that has been magnetically saturated parallel or antiparallel to the easy $[1\bar{1}1]$ direction (either up or down) by a current pulse through the C-shaped electromagnet. Lifetime techniques are used to measure an asymmetry, A_T, in the oPs formation rate. The polarization of the e^+ captured near or at the surface to form oPs is then deduced from the relation

$$A_T = (1/3)(\boldsymbol{P}_{e^+} \cdot \boldsymbol{P}_{e^-}).$$

Using this relation, the spin polarization of captured electrons at room temperature on Ni(110) is found to be $P_{e^-} = +(2.5 \pm 0.3)\%$ (majority spin) but is of opposite sign on Ni(100) where $\boldsymbol{P}_{e^-} = -(0.9 \pm 0.1)\%$ (minority spin). The size of A_T is reduced an order of magnitude by submonolayer coverage of oxygen or Cs, as well as Ar-ion sputtering, showing the technique's surface sensitivity. The temperature dependence of A_T (and thus P_{e^-}) was measured in the temperature

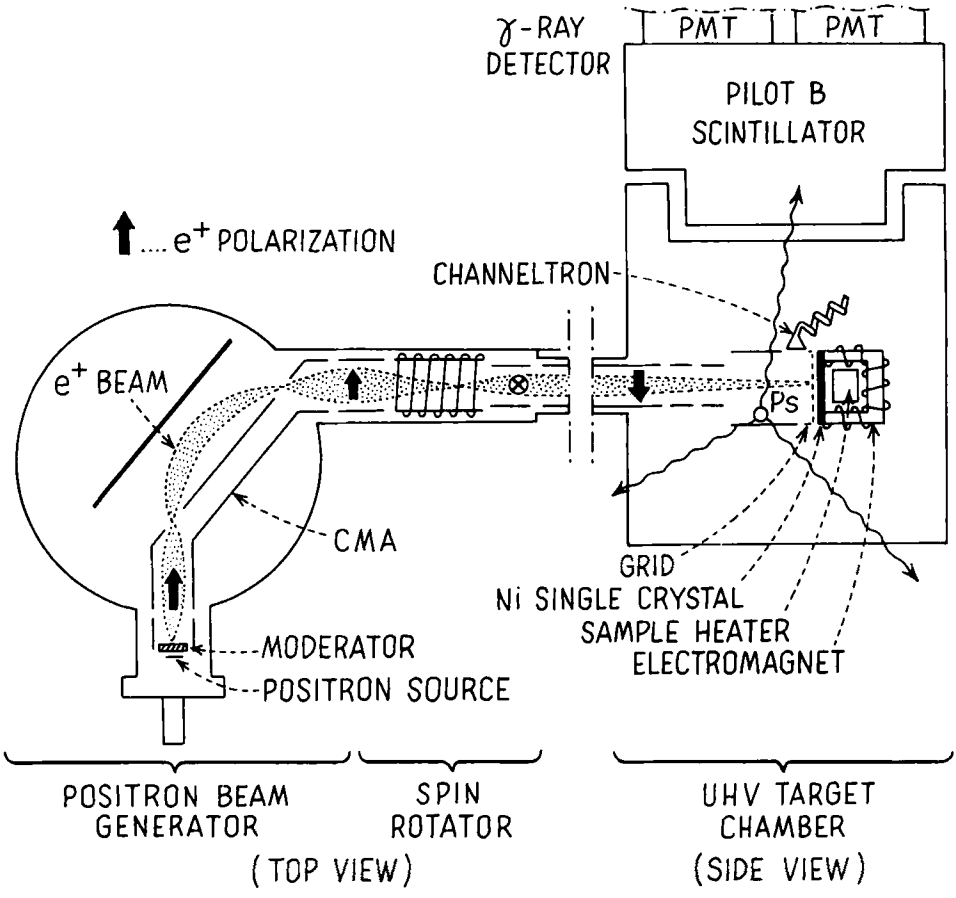

Fig. 5. Low-energy e^+ beam used to measure surface magnetism. Details of target chamber rotated 90° for clarity.

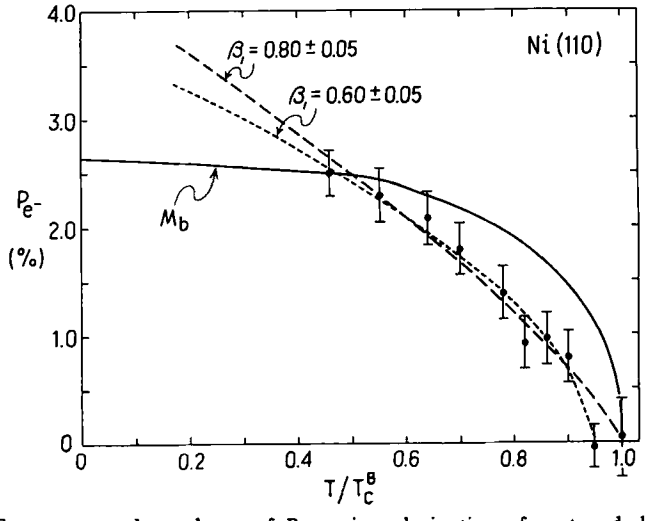

Fig. 6. Temperature dependence of P_{e^-}, spin polarization of captured electrons.

range $0.46 \leqslant T/T_c \leqslant 1.0$, where $T_c = 633$ K is the Ni Curie temperature (see fig. 6). A power law fit yields an effective critical exponent of 0.80 ± 0.05 which is in agreement with calculations as well as the results of a polarized electron scattering experiment (see references in ref. [5]). The exponent is more than a factor of two larger than the bulk critical exponent of Ni. Thus the technique shows promise as a quantitative probe of magnetic surface critical phenomena.

Additional surface magnetism studies of P_{e^-} in single crystals of Fe and Co are planned. It should also be possible to measure P_{e^-} in certain thin (1–5 monolayer) magnetic films epitaxially grown on either a magnetic or non-magnetic substrate. With the implementation of brightness enhanced, time-tagged e^+ beams of high intensity, the energy of oPs formed at the surface can be resolved by time-of-flight techniques [10]. This information will reveal the location in the density of states from which the captured electron originated. Understanding of the nature of Ps formation at surfaces will also be enhanced by these studies.

4.3. BULK MAGNETIZATION STUDIES

Information can also be obtained about the interactions of polarized low-energy e^+ with the electrons bound in the bulk of magnetic materials. Magnetic materials are used for constructing a moderator and the polarization of the low-energy e^+ emitted from the moderator surface is compared to the initial polarization of the β^+ injected into the material. A fractional depolarization of order $\Delta P/P = \omega_B \tau/2\pi$ will occur, where $\omega_B = eB_B/mc$ is the cyclotron frequency of electrons in the bulk magnetic field B_B and τ is the e^+ thermalization and diffusion time. A measurement of the polarization of low-energy e^+ emitted from a silicon steel moderator with randomly oriented domains shows $\Delta P/P = 0.4$. Using $B_B = 0.22$ T, we obtain $\tau = 65$ ps. This measurement has been confirmed by a recent measurement of the net circular polarization of the gammas resulting from e^+ annihilation within the bulk.

More quantitative results, allowing discrimination between diffusion and thermalization time, could be obtained by injecting a polarized e^+ beam into a magnetic single crystal and analyzing the phase shifts and amplitude reduction in the spin rotator curve as a function of incident e^+ energy.

4.4. INTERACTIONS WITH OPTICALLY ACTIVE MOLECULES

Many of the molecules that are the fundamental building blocks of living organisms are optically active (chiral) and, in fact, exhibit a macroscopic parity asymmetry in that essentially only L-amino acids and D-sugars are present in living organisms. It has been postulated (the Vester-Ulbricht hypothesis) that a causal connection exists between this phenomenon and the parity violation that occurs in nuclear β decay.

Chiral molecules have recently [11] been predicted to have a new property, a non-zero helicity per unit volume of the outer electrons. This electron helicity

density has two consequences. First, when low-energy e^+ with longitudinal polarization (helicity) form Ps in the L or D isomers, an asymmetry (A_{Ps}) is predicted to occur in the oPs formation fraction upon either reversal of the e^+ helicity or the exchange of the isomers. This asymmetry is predicted to be of the order of $10^{-8} < A_{Ps} < 10^{-6}$ for 100% longitudinally polarized, 100–200 eV e^+ incident on carbon-based targets. Second, when longitudinally polarized electrons are incident on the molecules the ionization rates of L and D molecules are predicted to exhibit an asymmetry, A_R. This asymmetry is estimated to be in the range $10^{-17} < A_R < 10^{-11}$ for β sources that could have been present on the early earth [12]. New theoretical work [13] on auto-catalysis shows that even very small biases toward one isomer could have overcome random fluctuations in the numbers of isomers so that the parity-violating weak interaction could have been the source of the macroscopic violation of parity in living organisms.

An experimental exploration of helicity density [8] uses oPs formation asymmetry (A_{Ps}) from low-energy e^+ because it is a factor of 10^5 larger than the asymmetry (A_R) predicted for high energy beta-electrons, and because polarized

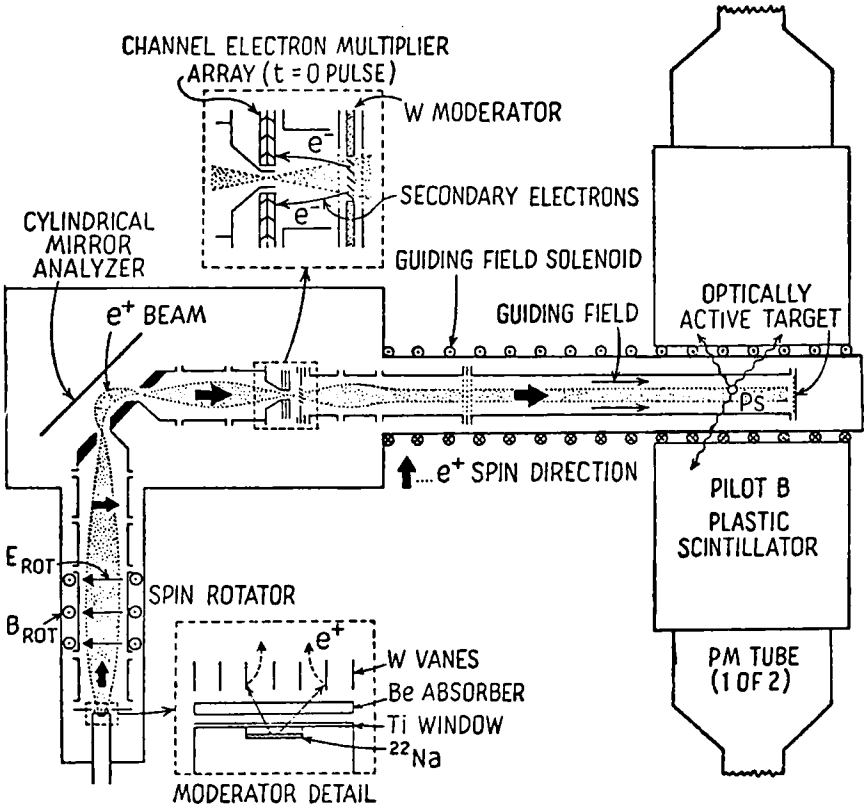

Fig. 7. Apparatus used to measure oPs formation asymmetries in optically active targets. Inset shows detail of source-moderator geometry.

Table 1
Experimental limits for orthopositronium formation asymmetries in chiral molecules [10].

Target	Z	$A_{Ps}(DL)\times10^{-4}$	$A_{Ps}(L)\times10^{-4}$	$A_{Ps}(D)\times10^{-4}$
Leucine	6	-0.5 ± 1.5	-1.2 ± 1.5	-2.7 ± 1.5
Selenocystine	34	$+0.1\pm4.1$	-9.0 ± 4.6	$+1.4\pm4.6$
Thyroxine	53	-5.9 ± 4.5	$+5.0\pm5.1$	$+1.3\pm5.0$

e^+ beams and Ps lifetime techniques permit the detection of very small asymmetries. In the experimental apparatus (fig. 7) a polarized ($P = 0.48$) low-energy e^+ beam is directed onto a target of amino acid powder. Calculations show that the beam helicity is partially preserved as the e^+ slow down to Ps formation energies. The value of A_{Ps} is measured by determining the fraction of e^+ forming the long lived (140 ns) oPs upon helicity reversal. The apparatus permits measurements of asymmetries as small as 1×10^{-4}, as shown in table 1. Theory predicts that $A_{Ps} \propto Z^2$, prompting the use of target materials with Z as high as 53 to increase the size of the asymmetry to measurable values. Note that we expect $A_{Ps}(DL) = 0$ and $A_{Ps}(L) = -A_{Ps}(D)$. Part of the theoretical range in high-Z materials is already excluded by the data in table 1. An improved apparatus, now undergoing final tests, will have a sensitivity of 1×10^{-5}.

4.5. POLARIZED ANTIPROTON PRODUCTION

In order to do polarized antiproton ($\bar{p}$) scattering experiments, a method to polarize $\bar{p}$ efficiently must be found. A possible method of achieving polarization [14,15] is via antihydrogen ($\overline{H}$) formation [16]

$$e^+ + \bar{p} \rightarrow \overline{H} + \gamma.$$

If the positron is polarized either before formation of the $\overline{H}$ or after by optical pumping, then the polarization can be transferred to the $\bar{p}$ via the hyperfine interaction. Consider $\overline{H}$ formation from a fully polarized e^+ beam ($\uparrow_{e^+}$) and an unpolarized $\bar{p}$ beam (50% $\uparrow_{\bar{p}}$, 50% $\downarrow_{\bar{p}}$). Half of the $\overline{H}$ would be formed in the state with $\uparrow_{e^+}\downarrow_{\bar{p}}$. The hyperfine interaction mixes the $\uparrow_{e^+}\downarrow_{\bar{p}}$ and $\downarrow_{e^+}\uparrow_{\bar{p}}$ states. Thus, after several hyperfine periods, the time-averaged $\bar{p}$ and e^+ polarization of these $\overline{H}$ would be zero. On the other hand, the half of the $\overline{H}$ formed in the $\uparrow_{e^-}\uparrow_{p^-}$ state would remain unaffected by the hyperfine interaction. The final $\bar{p}$ (and e^+) polarization is half that of the original e^+ polarization. Transfer of the entire e^+ polarization to the $\bar{p}$ can be achieved by the Sona method [17]. In any method, the e^+ would then be stripped away by passing the $\overline{H}$ through a thin foil, leaving the polarized $\bar{p}$.

We envision a first arrangement wherein positrons from a 400 GBq (10 Ci) ^{22}Na radioactive source are accumulated [18,19], stored in a small positron storage ring, and merged in an interaction region with the $\bar{p}$ in LEAR.

With one stage of brightness enhancement [20,21] to reduce the beam diameter to 1 mm, the projected positron density at a polarization $P = 0.15$ is $n_{e^+} = 2 \times 10^5$ cm^{-3}. Using the method of section 3, an e^+ polarization of $P = 0.50$ can be achieved, but the final e^+ density in the interaction region would drop [7] to 5×10^4 cm^{-3}. This would result in $\bar{p}$ with 25% polarization (using the hyperfine effect only) at an $\overline{H}$ production rate given by [22]:

$$R_{\overline{H}} = \eta \gamma^{-2} N_{\bar{p}} n_{e^+} \alpha$$

$$= (0.04)(1.06)^{-2}(10^{10})(5 \times 10^4)(2 \times 10^{-12}) = 40 \text{ s}^{-1}$$

where η is the fraction of the LEAR ring overlapped by the e^+ beam, $N_{\bar{p}}$ is the number of $\bar{p}$ that can be confined in a 1 mm diameter region at LEAR (a quantity limited by space charge), and α is the recombination coefficient for the process. Care must be taken to avoid depolarization of the $\overline{H}$ while passing through the LEAR focusing and bending magnets. After stripping the positron, the net result is 3×10^7, 25% polarized $\bar{p}$ per day in an extracted beam.

With such a polarized $\bar{p}$ beam one could measure asymmetries in polarized $\bar{p}$ scattering from polarized and unpolarized p targets in reactions such as:

$$\bar{p} + p \rightarrow \begin{cases} \bar{p} + p \\ \pi^+ + \pi^- \\ K^+ + K^- \\ \bar{n} + n. \end{cases}$$

Moreover one could study the asymmetry in the total cross-section given by

$$A_{\parallel} = \frac{1}{P_{\bar{p}} P_p} \left[\frac{\sigma_T(\uparrow_{\bar{p}} \uparrow_p) - \sigma_T(\downarrow_{\bar{p}} \uparrow_p) - \sigma_T(\uparrow_{\bar{p}} \downarrow_p) + \sigma_T(\downarrow_{\bar{p}} \downarrow_p)}{\sigma_T(\uparrow_{\bar{p}} \uparrow_p) + \sigma_T(\downarrow_{\bar{p}} \uparrow_p) + \sigma_T(\uparrow_{\bar{p}} \downarrow_p) + \sigma_T(\downarrow_{\bar{p}} \downarrow_p)} \right]$$

where $P_{\bar{p}}$ and P_p are the longitudinal polarizations of the antiproton beam and proton target, respectively, and the σ_T are the measured total cross sections with the sense of polarizations indicated by the arrows. A similar asymmetry $A_{\perp}$ could be measured for the p and $\bar{p}$ polarized transversely to the incident $\bar{p}$ direction. Each asymmetry could be measured to a precision [23]

$$\delta(A) = \frac{1}{\sqrt{N_{\text{event}}} P_{\bar{p}} P_p}$$

where N_{event} is the total number of $\bar{p}$ interacting in the target. If the target thickness is chosen so that 20% of the incident $\bar{p}$ interact in the target (a sufficiently small fraction to avoid degradation of the asymmetry by multiple scattering events) and given $P_{\bar{p}} = 0.25$ and the effective proton polarization in a hydrocarbon target with 70% hydrogenic proton polarization is typically $P_p = 0.12$ [24], then in one day of running one can attain

$$\delta(A) = \pm \frac{1}{\sqrt{0.2 \times 3 \times 10^7}\, 0.25 \times 0.12} = \pm 0.01.$$

By way of comparison, $A_{\parallel}$ is 0.15 for polarized pp scattering [25] at $P_{\mathrm{lab}} = 1.5$ GeV/c. Thus significant measurements of $A_{\parallel}$ and $A_{\perp}$ should result from these total cross section experiments. Measurements of differential cross sections for specific reaction channels would yield different information but would require longer data acquisition times due to their smaller event rates.

If the e^+ accumulation time can be increased to as long as 200 s (by use of the technique discussed in ref. [18] or by use of electron cooling of the e^+ during accumulation), then a density of $n_{e^+} = 10^8\,\mathrm{cm}^{-3}$ at $P = 0.5$ would be available for $\overline{\mathrm{H}}$ formation. This density is the space charge limit for a 1 mm diameter e^+ beam in a confining magnetic field. The resulting $\overline{\mathrm{H}}$ formation rate $R_{\overline{\mathrm{H}}} = 10^5\,\mathrm{s}^{-1}$ would convert all 10^{10} $\bar{\mathrm{p}}$ initially stored in LEAR to 25% polarized $\bar{\mathrm{p}}$ in one day. This would allow much smaller spin dependent cross sections for specific reaction channels to be measured.

4.6. TESTS OF DISCRETE SYMMETRIES

We have completed a preliminary experiment [9] that measures an angular correlation in the decay of polarized Ps. If the amplitude of this correlation, C_{n}, defined below, is non-zero, then CPT is violated. This experiment makes the first explicit use of polarized Ps.

The angular correlation, originally proposed by Bernreuther and Nachtmann [26] is:

$$C_{\mathrm{n}}\left[\hat{\boldsymbol{S}}\cdot\hat{\boldsymbol{k}}_1\times\hat{\boldsymbol{k}}_2\right],$$

where $\boldsymbol{S}$ is the triplet Ps spin, $|\boldsymbol{k}_1| > |\boldsymbol{k}_2| > |\boldsymbol{k}_3|$ are the momenta of the three decay γ rays, and $\hat{\boldsymbol{k}}_1\times\hat{\boldsymbol{k}}_2$ is in the direction of the normal to the γ-decay plane. Polarized Ps was produced using a polarized slow e^+ beam incident on a MgO-covered CEMA plate. The Ps was confined in an 11 cm^3 MgO-lined cavity and three NaI scintillators detected the decay γ-rays.

The final result for C_{n}, including both statistical and systematic errors, was found to be

$$C_{\mathrm{n}} = +0.020 \pm 0.023,$$

consistent with CPT invariance. We believe that systematic effects present in this first experiment may be reduced sufficiently, so that when combined with straight-forward improvements in the apparatus, a measurement of C_{n} to an accuracy thirty times better than our present results can be obtained.

Other discrete symmetry tests using spin aligned Ps, including tests of T invariance, are possible. In particular, a non-zero amplitude for the T-odd, P-odd, C-even angular correlation:

$$(\boldsymbol{S}\cdot\boldsymbol{k}_1)(\boldsymbol{S}\cdot\boldsymbol{k}_1\times\boldsymbol{k}_2)$$

would imply a T violation and a CP violation, but not necessarily a CPT violation. An experiment to measure this correlation is now under consideration.

Acknowledgments

The work reported in this article is supported by the National Science Foundation under grant PHY-8403817, by the Richard Wood Company, and by The University of Michigan.

References

[1] P.W. Zitzewitz, J.C. Van House, A. Rich and D.W. Gidley, Phys. Rev. Lett. 43 (1979) 1281.
[2] A. Rich, Rev. Mod. Phys. 53 (1981) 127; and references therein.
[3] C. Bouchiat and J.M. Levy-Leblond, Nuovo Cimento 33 (1964) 193.
[4] G. Gerber, D. Newman, A. Rich and E. Sweetman, Phys. Rev. D 15 (1977) 1189.
[5] D.W. Gidley, A. Köymen and T.W. Capehart, Phys. Rev. Lett. 49 (1982) 1779.
[6] A.R. Kömen, PhD Thesis, The University of Michigan (1985) (available from University Microfilms).
[7] J. Van House and P.W. Zitzewitz, Phys. Rev. A 29 (1984) 96.
[8] D.W. Gidley, A. Rich, J. Van House and P.W. Zitzewitz, Nature 297 (1982) 639.
[9] B.K. Arbic, S. Hatamian, M. Skalsey, J. Van House and W. Zheng, Phys. Rev. A 37 (1988) 3189.
[10] J. Van House, A. Rich and P.W. Zitzewitz, Origins of Life 16 (1986) 81.
[11] R. Hegstrom, Nature 197 (1982) 643.
[12] R. Hegstrom, A. Rich and J. Van House, Nature 313 (1985) 391.
[13] D.K. Kondepudi and G.W. Nelson, Nature 314 (1985) 438.
[14] R.S. Conti and A. Rich, in: *Low Energy Antimatter*, ed. D.B. Cline (World Scientific, Singapore, 1986).
[15] K. Imai, *Particles and Fields Series*, eds. A.D. Krisch, A.M.T. Lin and O. Chamberlain (1985) 229.
[16] H. Herr, D. Möhl and A. Winnacker, in: *Proc. 2nd Workshop on Physics with Cooled Low Energy Antiprotons at LEAR*, eds. U. Gastaldi and R. Klapisch (Plenum, New York, 1985).
[17] P.G. Sona, Energia Nucleare 14 (1967) 295.
[18] R.S. Conti, W. Frieze, D. Gidley, A. Rich, M. Skalsey, J. Van House, P.W. Zitzewitz, K. Lynn, H. Haseroth, C.E. Hill, J.-L. Vallet, J. Berger, P. Blatt, P. Hauck, W. Meyer, R. Neumann, H. Poth, B. Seligmann, W. Schwab, M. Woertge and A. Wolf, To be published in the Proceedings of the IV LEAR Workshop, Villars Switzerland, September 7-14, 1987.
[19] R. Conti et al., poster at this conference.
[20] W.E. Frieze, D.W. Gidley and K.G. Lynn, Phys. Rev. B 31 (1985) 5628.
[21] A.P. Mills, Jr., Appl. Phys. 22 (1980) 273.
[22] R. Neumann, H. Poth, A. Winnacker and A. Wolf, Z. Phys. A 313 (1983) 253.
[23] O. Chamberlain, *Particles and Fields Series*, ed. A.D. Krisch, A.M.T. Lin and O. Chamberlain (1985) 51.
[24] A. Krisch, University of Michigan, Private communication.
[25] O. Chamberlain, *Particles and Fields Series*, eds. A.D. Krisch, A.M.T. Lin and O. Chamberlain (1985) 26.
[26] W. Bernreuther and O. Nachtmann, Z. Phys. C 11 (1981) 235.